






Merger of a Neutron Star with a Black Hole: One-family versus Two-families Scenario

Francesco Di Clemente^{1,2} , Alessandro Drago^{1,2} , and Giuseppe Pagliara^{1,2} 

¹Dipartimento di Fisica e Scienze della Terra dell'Università di Ferrara, Via Saragat 1, I-44122 Ferrara, Italy

²INFN Sezione di Ferrara, Via Saragat 1, I-44122 Ferrara, Italy

Received 2021 July 11; revised 2022 March 4; accepted 2022 March 10; published 2022 April 12

Abstract

A kilonova (KN) signal is generally expected after a black hole–neutron star merger. The strength of the signal is related to the equation of state of neutron star matter, and it increases with the stiffness of the latter. The recent results obtained by NICER from the analyses of PSR J0740+6620 suggest a rather stiff equation of state, and the expected KN signal is therefore strong, at least if the mass of the black hole does not exceed $\sim 10 M_{\odot}$, the adimensional spin parameter is not too small, and the orbit is prograde. We compare the predictions obtained by considering equations of state of neutron star matter satisfying the most recent observations and assuming that only one family of compact stars exists with the results predicted in the two-families scenario. In the latter a soft hadronic equation of state produces very compact stellar objects, while a rather stiff quark matter equation of state produces massive strange quark stars, satisfying NICER results. The expected KN signal in the two-families scenario is very weak: in particular, the hadronic star–black hole merger produces a much weaker signal than in the one-family scenario because the hadronic equation of state is very soft. Moreover, according to the only existing simulation, the strange quark star–black hole merger does not produce a KN signal because the amount of mass ejected is negligible. These predictions will be easily tested with the new generation of detectors if black holes with an adimensional spin parameter $\chi_{\text{BH}} \gtrsim 0.2$ or a mass $M_{\text{BH}} \lesssim 4 M_{\odot}$ can be present in the merger.

Unified Astronomy Thesaurus concepts: Neutron stars (1108); Compact objects (288); Stellar mergers (2157); Nuclear physics (2077); Black holes (162); Stellar mass black holes (1611)

1. Introduction

Black hole–neutron star (BH–NS) mergers are astrophysical phenomena of great interest because they not only produce gravitational-wave (GW) signals but also can have very energetic electromagnetic (EM) counterparts in the form of short gamma-ray bursts (sGRBs) and kilonova (KN) explosions (Shibata & Taniguchi 2008). The disruption of the NS produces the dynamical ejection of some material and the formation of a disk of hot matter around the BH, and, in turn, these processes can be at the origin of an sGRB and a KN signal. In order to produce these EM signals, the BH should not be too massive; otherwise, it is not possible to form an accretion disk and to eject material. Instead, when the BH mass is $\lesssim 10 M_{\odot}$, the adimensional spin parameter is sufficiently high, and the equation of state (EOS) of the compact star is not too soft, a mass up to a few hundredths of a solar mass is dynamically ejected and a larger mass, up to a few tenths of a solar mass, forms an accretion disk that can later be ablated by the neutrinos, allowing a further ejection of mass.

It is very important to note that the latest results from the NICER analyses of PSR J0740+6620 indicate that the EOS of NS matter is rather stiff, at least for the most massive compact stars (Miller et al. 2021; Raaijmakers et al. 2021; Riley et al. 2021). If only one family of compact stars exists, we can therefore expect a strong KN signal associated with many BH–NS mergers.

In the two-families scenario the phenomenology of BH–NS mergers can be rather different. Within that scenario, outlined in Drago et al. (2014a), hadronic stars (HSs) and strange quark

stars (Qs) coexist; the EOS of hadronic matter is rather soft owing to the formation of hyperons and delta resonances at densities larger than about twice nuclear saturation density. In turn, this allows for the existence of HSs having small radii and a mass not exceeding $\sim 1.6 M_{\odot}$. The EOS of quark matter, instead, can be rather stiff, and the Qs branch is populated by large and massive objects, having masses that can potentially reach $2.6 M_{\odot}$ (see Bombaci et al. 2021).

In the two-families scenario a key assumption is the validity of the Bodmer–Witten hypothesis on the absolute stability of strange quark matter. Namely, at zero pressure strange quark matter is more bound than iron. In turn, this implies that hadronic matter is metastable and “decays,” under certain conditions, into strange quark matter. The conditions for such a conversion are related to the amount of strangeness that is present in hadronic matter (Bombaci et al. 2004; Drago et al. 2014a). In De Pietri et al. (2019) it has been estimated that only when the hyperon fraction exceeds ~ 0.1 can the quark phase start to be produced via nucleation. This occurs at densities of a few times the saturation density. Thus, HSs with a central value below this threshold are actually stable. Only HSs with larger values of the central density can convert into strange Qs. In this scenario, therefore, HSs and Qs coexist and populate two different branches of compact stars. The possibility of forming a QS with a radius larger than that of the HS having the same baryonic mass is a special feature of the two-families scenario, and the underlying dynamics have been clarified in many papers and in particular in Drago & Pagliara (2020).

In the two-families scenario the outcome of the merger of a BH and a compact star clearly depends on the nature of the low-mass companion. If the low-mass companion is a QS, the numerical simulations of Kluzniak & Lee (2002) suggest that no significant amount of material is dynamically ejected or left in the accretion torus.



Original content from this work may be used under the terms of the [Creative Commons Attribution 4.0 licence](https://creativecommons.org/licenses/by/4.0/). Any further distribution of this work must maintain attribution to the author(s) and the title of the work, journal citation and DOI.

The two-families scenario has been developed in order to account for the possible existence of very compact stars, having a radius $\lesssim 11.5$ km for a mass of $\sim 1.4\text{--}1.5 M_{\odot}$. It has been shown (see, e.g., Most et al. 2018) that it is not possible to obtain such small radii in the absence of a strong phase transition as that present in the two-families scenario. This scenario therefore becomes phenomenologically irrelevant if all compact stars have radii $\gtrsim 11.5$ km. Since the direct measurement of radii is nontrivial and is affected by large systematic errors, it is important to find alternative ways to test the existence of stars with very small radii. This is the aim of this paper, in which we show that stars having very small radii produce a significantly suppressed KN signal.

In this paper we will compare the predictions for the KN signal generated in a BH–NS merger by assuming either that:

1. only one family of NSs exists and that it satisfies the most recent observational constraints, or that
2. two families of compact stars exist and the merger of the BH is with a HS (first family), since the QS–BH merger will be assumed not to generate a KN.

2. Semianalytical Model

In order to get an estimate of the mass ejected, we use the semianalytical models of Barbieri et al. (2020), Foucart et al. (2018), and Kawaguchi et al. (2016), which provide a fit to the data obtained in the simulations of BH–NS mergers. The models allow us to estimate the mass of the disk M_{disk} and the dynamical ejecta mass M_{dyn} in terms of five quantities: the mass, compactness, and tidal deformability of the NS (M_{NS} , C_{NS} , and Λ_{NS}) and the mass and the parallel spin component of the BH (M_{BH} and $\chi_{\text{BH},\parallel}$). Once M_{disk} and M_{dyn} are estimated, it is possible to predict the strength of the KN signal (Barbieri et al. 2020).

The total mass of matter not immediately absorbed by the BH, M_{out} , is the sum of two components: M_{disk} , representing the gravitationally bound material, and M_{dyn} , the unbound part. M_{out} is given by an interpolation formula as (Foucart et al. 2018)

$$M_{\text{out}} = M_{\text{NS}}^b \left[\max \left(\alpha \frac{1 - 2\rho}{\eta^{1/3}} - \beta \tilde{R}_{\text{ISCO}} \frac{\rho}{\eta} + \gamma, 0 \right) \right]^{\delta}, \quad (1)$$

where α , β , γ , and δ are fitting parameters. In the analyses of Foucart et al. (2018) they make use of the so-called symmetric mass ratio, and in this way the parameterization remains stable even for masses of the BH and of the NS that are comparable. Notice also that in our analyses we are using mass ratios well inside the range of validity of the parameterization obtained in Foucart et al. (2018). Therefore, there is no dependence of the value of the parameters on the NS mass.

In the formula above M_{NS}^b is the NS baryonic mass and $\rho = (15\Lambda_{\text{NS}})^{-1/5}$ is a function of the tidal deformability Λ_{NS} . η is the symmetric mass ratio defined as

$$\eta = q/(1 + q)^2, \quad (2)$$

where $q = M_{\text{NS}}/M_{\text{BH}}$ is the mass ratio. $\tilde{R}_{\text{ISCO}} = R_{\text{ISCO}} c^2/GM_{\text{BH}}$ is the dimensionless innermost stable circular orbit (ISCO). This quantity is defined in Bardeen et al.

(1972) as

$$\tilde{R}_{\text{ISCO}}(\chi) = 3 + Z_2(\chi) - \text{sgn}(\chi) \sqrt{(3 - Z_1(\chi))(3 + Z_1(\chi) + 2Z_2(\chi))}, \quad (3)$$

where

$$Z_1(\chi) = 1 + (1 - \chi^2)^{1/3}[(1 + \chi)^{1/3} + (1 - \chi)^{1/3}] \quad (4)$$

and

$$Z_2(\chi) = (3\chi^2 + Z_1(\chi)^2)^{1/2}. \quad (5)$$

In Equation (1) parameters are fixed and do not depend on the NS mass, since the contribution of this mass is encoded in ρ and η . Moreover, R_{ISCO} is the BH ISCO, since in the original derivation the behavior of the unbound material is extrapolated assuming $M_{\text{BH}}/M_{\text{NS}} \rightarrow \infty$.

The dynamical ejecta mass is instead approximated by

$$M_{\text{dyn}} = M_{\text{NS}}^b \{ \max [a_1 q^{-n_1} (1 - 2C_{\text{NS}}) / C_{\text{NS}} + a_2 q^{-n_2} \tilde{R}_{\text{ISCO}}(\chi_{\text{BH},\parallel}) + a_3 (1 - M_{\text{NS}}/M_{\text{NS}}^b) + a_4, 0] \}, \quad (6)$$

where a_1 , a_2 , a_3 , a_4 , n_1 , and n_2 are the fitting parameters. $\chi_{\text{BH},\parallel} = \chi_{\text{BH}} \cos \iota_{\text{tilt}}$ is the BH parallel spin component, which depends on the adimensional BH spin χ_{BH} and on ι , the angle between the BH spin and the total angular momentum. Notice that to have a large value for M_{dyn} the orbit must be prograde with respect to the BH spin. Here and in the following, we assume therefore prograde orbits, i.e., $\chi_{\text{BH},\parallel} \geq 0$. It is then possible to estimate the mass of the accretion disk as

$$M_{\text{disk}} = \max [M_{\text{out}} - M_{\text{dyn}}, 0], \quad (7)$$

i.e., the bound material is the total material outside the BH minus the gravitationally bound part.

Following Barbieri et al. (2020), we set the limit for the dynamical ejecta mass as

$$M_{\text{dyn,max}} = f M_{\text{out}}, \quad (8)$$

where f is the maximum ratio between the dynamical ejecta mass and the total mass outside the BH.

In conclusion, after an EOS for NS matter has been selected, both M_{disk} and M_{dyn} can be evaluated as functions of M_{NS} , M_{BH} , and χ_{eff} .

3. Observational Limits on the Equation of State

The recent results of NICER indicate rather large radii for masses ranging from ~ 1.4 up to $\sim 2 M_{\odot}$. In the left panel of Figure 1 we show a few recent limits on masses and radii, and in particular those obtained by NICER. As can be seen, EOSs that are moderately soft as SFHO are only marginally compatible with the data, which instead suggest either a stiff nucleonic EOS or a pure quark matter EOS (see Traversi et al. 2021). We also show two EOSs, 2B and SFHO+HD, which are NOT compatible with the limits presented in the figure. SFHO+HD is a hadronic EOS incorporating Δ -resonances and hyperons, and it is representative of the hadronic branch of the two-families scenario. The compact objects associated with this branch have small radii, as for the ones suggested, e.g., by Özel & Freire (2016) and Capano et al. (2020). 2B is a simple piecewise polytropic EOS (Markakis et al. 2009), and it has been used as a reference by Barbieri et al. (2020) to provide an

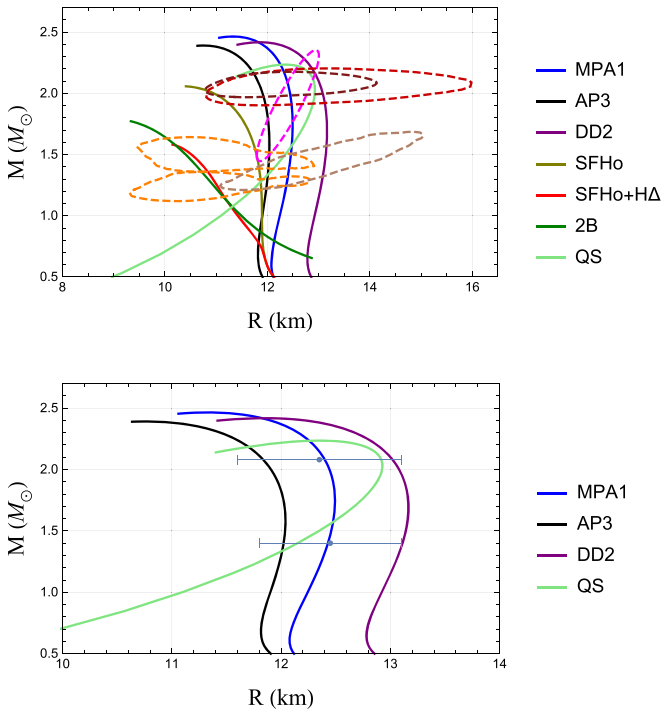


Figure 1. Top panel: observational limits on masses and radii of selected sources (dashed lines), compared with a few EOSs (solid lines). NICER results for PSR J0740+6620: brown from Riley et al. (2021) and dark red from Miller et al. (2021). Sepia: NICER results for PSR J0030+0451 from Riley et al. (2019). Violet: limits on 4U 1702-429 from Nättilä et al. (2017). Orange: limits from GW170817 from Abbott et al. (2018). Bottom panel: limits on the radius at 68% of the credibility interval for stars with masses 1.4 and 2.08 M_{\odot} based on the analysis of NICER results and on GW170817 (Miller et al. 2021), with three nucleonic EOSs (used in our analysis) and a QS. The nucleonic EOSs are MPA1 (Müther et al. 1987), DD2 (Typel et al. 2010), AP3 (Akmal et al. 1998), and SFHo (Steiner et al. 2013). SFHo+HD (Drago et al. 2014b) incorporates Δ -resonances and hyperons, and 2B is a soft piecewise polytropic EOS used as a reference (Markakis et al. 2009).

example of a soft EOS that does not produce a strong KN signal. It is important to notice that 2B is only slightly softer than SFHo+HD. In the right panel of Figure 1 we compare the limits obtained by Miller et al. (2021) with the results of three purely nucleonic EOSs that are representative of the range of values of radii compatible with the observations, if only one family of compact stars exists. Two of the EOSs, MPA1 and DD2, have been discussed also in Barbieri et al. (2020), while AP3 is close to the left limit indicated by Miller et al. (2021). It is important to recall that if only one family of compact stars exists, there is a rather precise linear relation between radius and tidal deformability of NSs having masses of about 1.5 M_{\odot} (Burgio et al. 2018), and therefore the limits on the radii directly translate into limits on the tidal deformability.

In Figure 2 we show the tidal deformabilities for a similar set of EOSs. Notice that the group of EOSs satisfying the limits of Miller et al. (2021) in the one-family case are rather well separated from SFHo+HD and 2B, EOSs that can be justified in a two-families scenario.

4. Predicted Values of M_{disk} and of M_{dyn}

In previous papers (Shibata & Taniguchi 2008; Barbieri et al. 2020) it has been shown that a strong KN signal can be obtained if the EOS is stiff, due to large values for M_{disk} and M_{dyn} . Here we compare the estimated values of these two masses, computed by assuming that only one family of

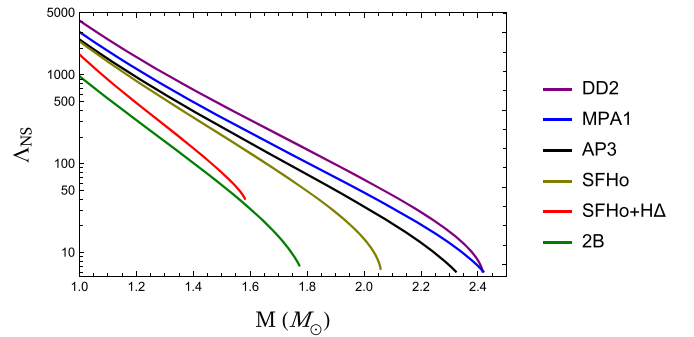


Figure 2. Tidal deformability for various representative EOSs as a function of the NS mass.

compact stars exists (and the EOS has therefore to satisfy limits of the type discussed in Miller et al. 2021), with the values obtained in the two-families scenario for the merger of an HS with a BH.

In Figure 3 we compare the results obtained by using MPA1 with those obtained using SFHo+HD, for $M_{\text{NS}} = 1.4 M_{\odot}$. Notice that the M - R relation based on MPA1 passes close to the central values obtained by the analysis of Miller et al. (2021), as shown in the bottom panel of Figure 1. For simplicity, we have assumed $\iota_{\text{tilt}} = 0$. It is clear from Figure 3 that when using MPA1 there exists a rather extended range of values of χ_{BH} and of M_{BH} , leading to large values of M_{disk} and M_{dyn} , and therefore to strong KN signals, while for the same values of χ_{BH} and of M_{BH} no mass is ejected if SFHo+HD is used. The difference is particularly strong and relevant for small values of M_{BH} ; for instance, if $M_{\text{BH}} = 4 M_{\odot}$, no disk forms when using SFHo+HD for $\chi_{\text{BH}} \lesssim 0.65$, while for MPA1 a disk forms for $\chi_{\text{BH}} \gtrsim 0.3$. If one examines M_{dyn} , the differences between the two scenarios are also present but less marked.

In Figure 4 we compare the one-family versus the two-families scenario considering the three nucleonic EOSs presented in the bottom panel of Figure 1: their M - R relations are representative of the entire range of values allowed by the analysis of Miller et al. (2021). For $M_{\text{NS}} \sim 1.2$ – $1.3 M_{\odot}$ when using SFHo+HD the amount of mass dynamically ejected is much smaller than in the one-family scenario, and it becomes 0 at 1.4 M_{\odot} .

5. Modeling Observations

5.1. A Toy Model to Mimic Correlations between Observables

GW observational data from LIGO-Virgo (LV hereafter) provide a fairly accurate measurement of the chirp mass, but not an equally accurate measurement of the spin and individual masses of the components of a merger. When performing the data analysis, the values of the masses and spins turn out to be strongly correlated. Therefore, we relied on a toy model developed in Ng et al. (2018), which provides synthetic posteriors in order to emulate the data analysis. The model shows how Gaussian and uncorrelated likelihoods for the symmetric mass ratio and the 1.5PN phase term (the quantity ψ described below) can result in a skewed posterior for the effective spin parameter of the binary system. The resulting

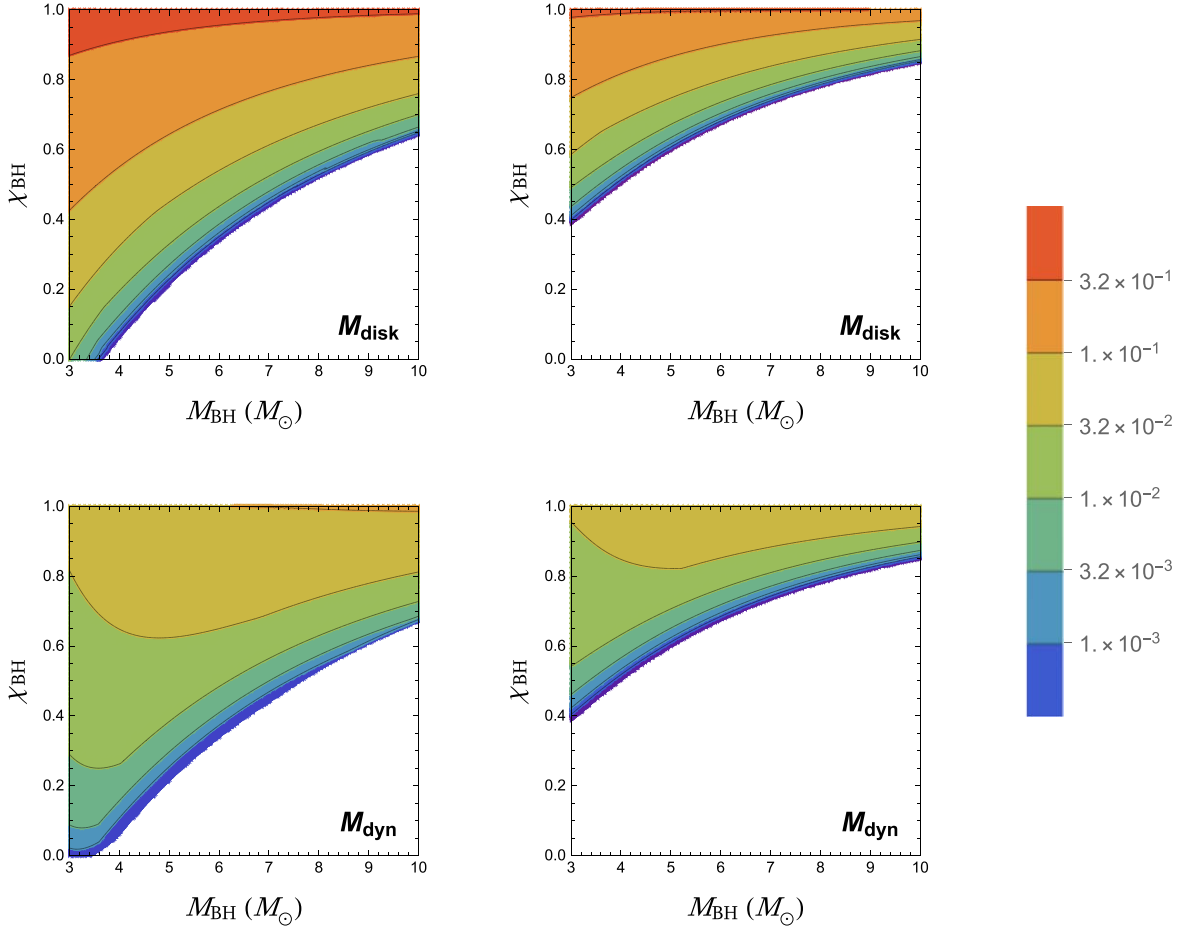


Figure 3. Plots for the mass of the disk on top and for dynamical ejecta on bottom. Left figures are relative to MPA1, right figures to SFHO+HD. The considered mass of the star is $\sim 1.4 M_{\odot}$. Values for tidal deformability for MPA1 and SFHO+HD are $\Lambda_{\text{NS}} \simeq 462$ and $\Lambda_{\text{NS}} \simeq 151$, respectively. Plots are a function of the BH mass (M_{BH}) and of the adimensional spin parameter χ_{BH} .

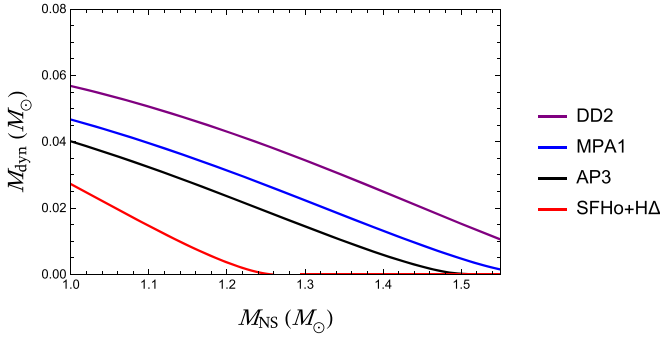


Figure 4. Dynamical ejecta mass for a BH of $5 M_{\odot}$ with a spin parameter $\chi = 0.4$, as a function of the NS mass.

likelihood for the masses and the effective spin parameter reads

$$\mathcal{L}(M_{\text{NS}}, M_{\text{BH}}, \chi_{\text{eff}}) = \mathcal{N}(\psi(M_{\text{NS}}, M_{\text{BH}}, \chi_{\text{eff}}); \psi_0, \sigma_{\psi}) \times \mathcal{N}(\eta(M_{\text{NS}}, M_{\text{BH}}); \eta_0, \sigma_{\eta}), \quad (9)$$

where the effective inspiral spin parameter is

$$\chi_{\text{eff}} = \left(\frac{M_{\text{NS}}}{M_{\text{NS}} + M_{\text{BH}}} \chi_{\text{NS}} + \frac{M_{\text{BH}}}{M_{\text{NS}} + M_{\text{BH}}} \chi_{\text{BH}} \right) \cdot \hat{L}, \quad (10)$$

in which \hat{L} is the unit vector along the orbital angular momentum and χ_{NS} and χ_{BH} are the NS and BH adimensional spin vectors. In Equation (9), $\mathcal{N}(x; x_0, \sigma_x)$ represents a

Gaussian in the variable x , centered in x_0 with standard deviation σ_x . The variable ψ is defined as

$$\psi = \eta^{-3/5} \left[\frac{(113 - 76\eta)\chi_{\text{eff}} + 76\delta\eta\chi_a}{128} - \frac{3\pi}{8} \right]. \quad (11)$$

In the formula above $\delta = (M_{\text{BH}} - M_{\text{NS}})/(M_{\text{BH}} + M_{\text{NS}})$ and $\chi_a = (\chi_{\text{BH},\parallel} - \chi_{\text{NS},\parallel})/2$, where $\chi_{\text{BH},\parallel}$ and $\chi_{\text{NS},\parallel}$ are the parallel components of the spins. The spin of the less massive body is neglected by setting $\chi_{\text{NS},\parallel} = 0$, so that

$$\chi_{\text{eff}} = \chi_{\text{BH},\parallel}/(1 + q) \quad (12)$$

and

$$\chi_a = (1 + q)\chi_{\text{eff}}/2. \quad (13)$$

Finally, in our analysis we have taken into account the observational constraint on the chirp mass by adding a multiplicative term to Equation (9):

$$\mathcal{L}_{\text{total}}(M_{\text{NS}}, M_{\text{BH}}, \chi_{\text{eff}}) = \mathcal{L}(M_{\text{NS}}, M_{\text{BH}}, \chi_{\text{eff}}) \times \mathcal{N}(M_{\text{chirp}}(M_{\text{NS}}, M_{\text{BH}}); M_{\text{chirp},0}, \sigma_{M_{\text{chirp}}}). \quad (14)$$

In our analyses, we identify an event by choosing the central values $M_{\text{NS},0}$, $M_{\text{BH},0}$, and $\chi_{\text{eff},0}$, and in this way we fix the values of ψ_0 , η_0 , and $M_{\text{chirp},0}$. The standard deviations σ_{ψ} , σ_{η} , and $\sigma_{M_{\text{chirp}}}$ have been fixed in order to approximate the correlations observed in LV analyses and displayed in Figures 4 and 8 of Abbott et al. (2021). In our Figure 5, the

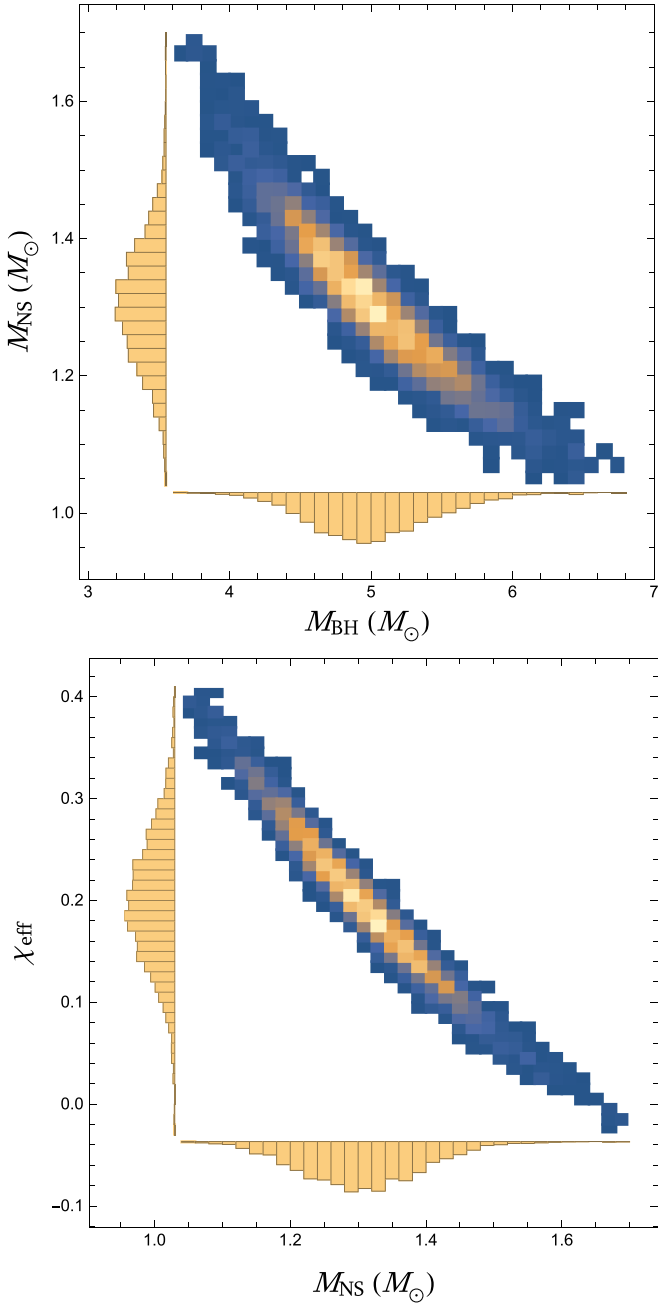


Figure 5. Example of correlations obtained with the toy model for an event characterized by the following values: $M_{\text{NS},0} = 1.3 M_{\odot}$, $M_{\text{BH},0} = 5 M_{\odot}$, $\chi_{\text{eff},0} = 0.2$, $\sigma_{\psi} = 0.005$, $\sigma_{\eta} = 0.015$, and $\sigma_{M_{\text{chirp}}} = 0.025$. Top: correlation between M_{NS} and M_{BH} . Bottom: correlation between M_{NS} and χ_{eff} .

marginalized distribution functions obtained with a Markov Chain Monte Carlo sampling of the likelihood of Equation (14) are shown.

5.2. Probability of Observing the Kilonova Signal

To calculate the luminosity of the possible KN signal, we rely on the model developed by Kawaguchi et al. (2016). Since we know the limiting magnitude per band of LSST (Vera Rubin Observatory; Chase et al. 2022), we can calculate for each event and for each EOS the probability of observing a KN signal. We set the distance of the hypothetical events at 200 Mpc, which is within the observing range of LV.

Table 1

Probability of Observing a KN Signal in the G Band by LSST after 1 day from the Merger Event, for Four EOSs at a Distance of 200 Mpc.

	SFHO+HD	AP3	MPA1	DD2
13ns5bh0c_1s	0.01	0.13	0.26	0.48
13ns5bh0c_05s	0.00	0.04	0.18	0.52
13ns7bh0c_1s	0.00	0.00	0.00	0.05
13ns7bh0c_05s	0.00	0.00	0.00	0.00
13ns5bh2c_1s	0.10	0.53	0.67	0.83
13ns5bh2c_05s	0.02	0.55	0.79	0.96
13ns7bh2c_1s	0.00	0.08	0.19	0.36
13ns7bh2c_05s	0.00	0.02	0.07	0.36
13ns5bh5c_1s	0.64	0.95	0.97	0.99
13ns5bh5c_05s	0.82	1.00	1.00	1.00
13ns7bh5c_1s	0.23	0.63	0.72	0.81
13ns7bh5c_05s	0.15	0.84	0.97	1.00

Note. The g -band limiting magnitude (AB) has been set at 24.7 with $\lambda_{\text{eff}} = 4830 \text{ \AA}$ following Chase et al. (2022). Labels of the event are in the format (NS mass $\times 10$) ns(BH mass) bh(effective spin $\times 10$) c_Xs, where if X is 1, we use the standard deviations inferred from LV analysis; if it is 05, they are halved.

The procedure we adopt is as follows: for each event we generate an ensemble of points according to Equation (14); for each generated point we compute M_{dyn} by using Equations (6) and (8); we then calculate the bolometric luminosities, the bolometric magnitudes, and the bolometric corrections³ for a single band filter (g -band filter); finally, we compute the fraction of the sample that generates a visible magnitude smaller than the limiting one of LSST, and in this way we obtain the probabilities displayed in Table 1.

6. Results and Conclusions

As shown in Table 1, the probability of observing a KN signal is negligible if the BH spin χ_{BH} is close to 0. For instance, the event *13ns7bh0c_1s* is similar to GW200115, and we can confirm the result of other authors (Abbott et al. 2021; Zhu et al. 2021) of a very low probability of observing a KN signal for that event even assuming a stiff EOS. Notice anyway that if the BH mass is very small ($\chi_{\text{BH}} \lesssim 5 M_{\odot}$) and the EOS of the NS is particularly stiff, a KN signal is expected even for nonrotating BHs.

While our paper was in preparation, two other works appeared discussing the probability of observing a KN signal in an NS–BH merger, Zhu et al. (2021) and Fragione (2021). It is important to clarify the differences in the approach followed in our work with respect to those papers. First, Zhu et al. (2021) discuss events generated by using the population synthesis code STARTRACK of Belczynski et al. (2008, 2020). In that way they conclude that χ_{BH} is smaller than about 0.2, and therefore the possibility of generating an observable KN signal is marginal. Fragione (2021) also makes use of various

³ The bolometric correction of a specific observational band is the difference between the bolometric magnitude and the visible magnitude in that band.

population synthesis results in order to estimate the probability of having mergers with given values of masses and spins, and from those values it estimates the probability of generating an observable KN signal. In our approach we do not use population synthesis, but we concentrate on the information that can be obtained from the realistic analysis of an event in which the extrapolated values of the masses and of the spin are correlated. The reason we do not make use of population synthesis is that in the existing codes the possibility of having an NS–BH merger from a hierarchical triple system is not included (G. Wiktorowicz 2021, private communication). On the other hand, the possibility of a merger originating from a triple system has been suggested, e.g., in connection with GW190814 (Lu et al. 2020; Liu & Lai 2021). If the BH participating in the NS–BH merger is obtained from a previous merger of two NSs, its mass can be small and it can be rapidly rotating. Therefore, in the analysis presented in Table 1 we also discuss BHs that are more rapidly rotating.

In order to take into account the predictable increase in the future sensitivity of LV detectors, we have considered in our analyses the possibility that the current average error (at the origin of the correlation between estimated masses and spin) will be halved. As shown in the table, the augmented precision makes it slightly more easy to discriminate among the various EOSs, but the improvement is not very significant.

The most important result of our analysis is that if the BH spin is not always vanishing, it is possible to discriminate among the various EOSs and, even more clearly, between the one-family scenario and the two-families scenario. As shown in the table (and also taking into account the dependence of M_{dyn} on the mass of the NS, shown in Figure 4), a rather strong KN signal is expected in the one-family scenario, in particular for $M_{\text{NS}} \sim 1.2\text{--}1.3 M_{\odot}$ and $M_{\text{BH}} \lesssim 5 M_{\odot}$, if $\chi_{\text{BH}} \gtrsim 0.2$. Moreover, if $M_{\text{BH}} \lesssim 4 M_{\odot}$ (as in the case of GW190425; Abbott et al. 2020), a strong KN signal is expected in the one-family scenario even for a nonrotating BH. Instead, in the two-families scenario and in most of the analyzed cases almost no mass escapes the BH. Notice also that the hadronic EOS we have used in our analysis is not the softest possible. In previous papers (see, e.g., Drago et al. 2014a) we have discussed even softer EOSs, which can explain HSs with even smaller radii, such as those suggested in Özel & Freire (2016), if their existence is confirmed. Therefore, an even weaker KN signal can be justified within the two-families scenario.

A caveat is in order: in our analysis we have assumed that no matter is ejected in a QS–BH merger, as suggested by Kluzniak & Lee (2002). However, in that simulation the gravity of the BH is modeled through a pseudo-Newtonian potential with an absorbing boundary corresponding to the radius of the photon orbit in Schwarzschild geometry. The results of Kluzniak & Lee (2002) therefore need to be confirmed by new and more sophisticated numerical simulations in full general relativity. On the other hand, our main prediction is that for compact stars having masses of about $1.2\text{--}1.3 M_{\odot}$, which in the two-families scenario are HSs, the KN signal is significantly suppressed with respect to the one-family case, and this prediction does not depend on the QS–BH simulation.



Obviously, also in NS–NS mergers it is possible to find clear signatures of the two-families scenario. As discussed in Drago & Pagliara (2018) and De Pietri et al. (2019), in the two-families scenario there are three types of mergers, namely, HS–HS, HS–QS, and QS–QS, and therefore the related

phenomenology is very rich. For instance, the threshold mass for obtaining a prompt collapse to a BH depends on the type of merger. While in the one-family scenario one does not expect to have a prompt collapse for masses smaller than the mass of the binary at the origin of GW170817 ($\sim 2.74 M_{\odot}$), in the two-families scenario (in which GW170817 was associated with an HS–QS merger) there could be a prompt collapse for masses just above $2.5 M_{\odot}$, if the binary is made of two HSs (see De Pietri et al. 2019). This is a unique prediction of the two-families scenario.

In conclusion, we have shown that the observation of the KN signal produced in an NS–BH merger can provide clear indications in favor or against the two-families scenario. The strongest discrimination between the “normal” scenario and the two-families scenario comes from mergers in which the masses of both the NS and the BH are rather small and $\chi_{\text{BH}} \gtrsim 0.2$, and these constraints reduce the number of mergers that can be used in the analysis. However, the next generation of telescopes and the next Ligo-VIRGO runs will be able to observe KN signals up to ~ 475 Mpc (Chase et al. 2022), thus significantly enlarging the observable volume. The analysis just released by Abbott et al. (2021) of two NS–BH mergers, GW200105 and GW200115, found that a small value of ejected mass was expected from both events, consistent with the absence of any EM counterpart. That same conclusion can be reached by analyzing the results we obtained in Figures 3 and 4 and using the estimated masses and spins of those two events. On the other hand, as suggested in Abbott et al. (2021), the detection of those two mergers indicates that the estimated rate for this type of event is realistic, and therefore we can expect, in the near future, to be able to gather crucial information from the search of KN signals from NS–BH mergers, unless the spin of all the BHs in an NS–BH merger is close to zero.

ORCID iDs

Francesco Di Clemente  <https://orcid.org/0000-0002-8257-3819>

Alessandro Drago  <https://orcid.org/0000-0003-1302-8566>
Giuseppe Pagliara  <https://orcid.org/0000-0003-3250-1398>

References

- Abbott, B. P., Abbott, R., Abbott, T. D., et al. 2020, *ApJL*, **892**, L3
 Abbott, B. P., Abbott, R., Abbott, T. D., et al. 2018, *PhRvL*, **121**, 161101
 Abbott, R., Abbott, T., Abraham, S., et al. 2021, *ApJL*, **915**, L5
 Akmal, A., Pandharipande, V. R., & Ravenhall, D. G. 1998, *PhRvC*, **58**, 1804
 Barbieri, C., Salafia, O. S., Perego, A., Colpi, M., & Ghirlanda, G. 2020, *EPJA*, **56**, 8
 Bardeen, J. M., Press, W. H., & Teukolsky, S. A. 1972, *ApJ*, **178**, 347
 Belczynski, K., Kalogera, V., Rasio, F. A., et al. 2008, *ApJS*, **174**, 223
 Belczynski, K., Klencki, J., Fields, C. E., et al. 2020, *A&A*, **636**, A104
 Bombaci, I., Drago, A., Logoteta, D., Pagliara, G., & Vidana, I. 2021, *PhRvL*, **126**, 162702
 Bombaci, I., Parenti, I., & Vidana, I. 2004, *ApJ*, **614**, 314
 Burgio, G. F., Drago, A., Pagliara, G., Schulze, H. J., & Wei, J. B. 2018, *ApJ*, **860**, 139
 Capano, C. D., Tews, I., Brown, S. M., et al. 2020, *NatAs*, **4**, 625
 Chase, E. A., O’Connor, B., Fryer, C. L., et al. 2022, *ApJ*, **927**, 163
 De Pietri, R., Drago, A., Feo, A., et al. 2019, *ApJ*, **881**, 122
 Drago, A., Lavagno, A., & Pagliara, G. 2014a, *PhRvD*, **89**, 043014
 Drago, A., Lavagno, A., Pagliara, G., & Pigato, D. 2014b, *PhRvC*, **90**, 065809
 Drago, A., & Pagliara, G. 2018, *ApJL*, **852**, L32
 Drago, A., & Pagliara, G. 2020, *PhRvD*, **102**, 063003
 Foucart, F., Hinderer, T., & Nissanke, S. 2018, *PhRvD*, **98**, 081501
 Fragnone, G. 2021, *ApJL*, **923**, L2
 Kawaguchi, K., Kyutoku, K., Shibata, M., & Tanaka, M. 2016, *ApJ*, **825**, 52
 Kluzniak, W., & Lee, W. H. 2002, *MNRAS*, **335**, L29

- Liu, B., & Lai, D. 2021, [MNRAS](#), **502**, 2049
- Lu, W., Beniamini, P., & Bonnerot, C. 2020, [MNRAS](#), **500**, 1817
- Markakis, C., Read, J. S., Shibata, M., et al. 2009, [JPhCS](#), **189**, 012024
- Miller, M. C., Lamb, F. K., Dittmann, A. J., et al. 2021, [ApJL](#), **918**, L28
- Most, E. R., Weih, L. R., Rezzolla, L., & Schaffner-Bielich, J. 2018, [PhRvL](#), **120**, 261103
- Müther, H., Prakash, M., & Ainsworth, T. 1987, [PhLB](#), **199**, 469
- Näätäjä, J., Miller, M. C., Steiner, A. W., et al. 2017, [A&A](#), **608**, A31
- Ng, K. K. Y., Vitale, S., Zimmerman, A., et al. 2018, [PhRvD](#), **98**, 083007
- Özel, F., & Freire, P. 2016, [ARA&A](#), **54**, 401
- Raaijmakers, G., Greif, S. K., Hebeler, K., et al. 2021, [ApJL](#), **918**, L29
- Riley, T. E., Watts, A. L., Ray, P. S., et al. 2021, [ApJL](#), **918**, L27
- Riley, T. E., Watts, A. L., Bogdanov, S., et al. 2019, [ApJL](#), **887**, L21
- Shibata, M., & Taniguchi, K. 2008, [PhRvD](#), **77**, 084015
- Steiner, A. W., Hempel, M., & Fischer, T. 2013, [ApJ](#), **774**, 17
- Traversi, S., Char, P., Pagliara, G., & Drago, A. 2021, [arXiv:2102.02357](#)
- Typel, S., Röpke, G., Klähn, T., Blaschke, D., & Wolter, H. H. 2010, [PhRvC](#), **81**, 015803
- Zhu, J.-P., Wu, S., Yang, Y.-P., et al. 2021, [ApJ](#), **921**, 156